Multimodality image integration for radiotherapy treatment, an easy approach

A Santos[a], J Pascau[b], M Desco[b], JA Santos[b], F Calvo[b], C Benito[b], P Garcia-Barreno[b]

[a]Universidad Politécnica de Madrid, E-28040 Madrid, Spain
[b]Hospital General Universitario 'G. Marañón', E-28007 Madrid, Spain

ABSTRACT

The interest of using combined MR and CT information for radiotherapy planning is well documented. However, many planning workstations do not allow to use MR images, nor import predefined contours. This paper presents a new simple approach for transferring segmentation results from MRI to a CT image that will be used for radiotherapy planning, using the same original CT format.

CT and MRI images of the same anatomical area are registered using mutual information (MI) algorithm. Targets and organs at risk are segmented by the physician on the MR image, where their contours are easy to track. A locally developed software running on PC is used for this step, with several facilities for the segmentation process. The result is transferred onto the CT by slightly modifying up and down the original Hounsfield values of some points of the contour. This is enough to visualize the contour on the CT, but does not affect dose calculations. The CT is then stored using the original file format of the radiotherapy planning workstation, where the technician uses the segmented contour to design the correct beam positioning.

The described method has been tested in five patients. Simulations and patient results show that the dose distribution is not affected by the small modification of pixels of the CT image, while the segmented structures can be tracked in the radiotherapy planning workstation –using adequate window/level settings-. The presence of the physician is not required at the planning workstation, and he/she can perform the segmentation process using his/her own PC.

This new approach makes it possible to take advantage from the anatomical information present on the MRI and to transfer the segmentation to the CT used for planning, even when the planning workstation does not allow to import external contours. The physician can draw the limits of the target and areas at risk off-line, thus separating in time the segmentation and planning tasks and increasing the efficiency.

Keywords: Radiotherapy planning, Magnetic Resonance Imaging, MR, Computer Tomography, CT, Radiotherapy, image registration, image segmentation

1.   CLINICAL BACKGROUND

Radiotherapy 3D planning consists of three-dimensional dosimetry of the target irradiation volume, reconstructed from the information obtained from computed tomography (CT) and/or magnetic resonance (MRI) images. 3D dosimetry planning has allowed the development of conformal therapy, which tries to match radiation beams to the asymmetric and irregular shapes of the target volume.

Several technological advances have contributed to optimize radiotherapy applications and the treatment quality: The use of special collimators, such as the 'multileaf' which totally conform the radiation field, the use of verification images obtained by digital reconstruction and the ability to control in real time the course of each session.

Correspondence: A. Santos: andres@die.upm.es; ETSI Telecomunicación, E-28040, Madrid, SPAIN. http://www.die.upm.es/im

From the clinical point of view, 3D planning and conformal radiotherapy have allowed to increase the radiation dose in the tumor volume without compromising the toxicity on critical organs [1]. This fact, based on the direct dose-response relation, allows increases of 15 to 25% over traditional standard total doses [2].

The aim of 3D planning is to adjust radiation beams to the shape of the volume to be treated, minimizing radiation to neighboring regions. Beam intensity modulation consists of manipulating the radiation beam, so that each beam reaches the patient with a different intensity. Several devices are used in order to improve the quality of the radiation process, such as multileaf collimators, virtual simulation or 3D planning. These systems take into account not only criteria based on dose limits, but also biological indexes. Computer controlled automation of multileaf collimators is the basis of this new radiotherapy treatment approach, which already appears as the essential way to improve quality of radiation.

CT is the standard modality for image acquisition of the irradiation field. It allows the definition of the field limits and the contour of the patient region where references are projected (tattoos, scars, fiducial markers) and to outline all interesting organs or tumors. An essential advantage of CT is that it provides information on tissue density, thus allows for the calculation of radiation doses. Most Radiation Oncology departments have a CT connected to planning workstations. Images are frequently transferred digitally from the CT scanner to the planning workstation, without the need of manually digitizing the film.

Nevertheless, the use of CT poses several drawbacks: Low image quality of soft tissues and in some anatomical locations such as the central nervous system (CNS); the inability, except in the case of modern helicoidal scanners, to obtain coronal slices or saggital image reconstructions. The allergy of some patients to iodine contrast agents is other problem that prevents from obtaining relevant data about tumor extension. For these reasons the use of combined information coming form different image modalities is an important improvement, recently introduced. The described disadvantages of CT images can be overcome with the addition of physiological and functional information about the tumor and its surroundings. This additional possibilities come from modalities like MRI or Positron Emission Tomography (PET)[3].

Recently published results remark the usefulness of MRI in correctly delimitating irradiation volumes and as an aid in the patient simulation in cases where anatomy has been altered by previous surgical procedures [4-7]. MRI provides a higher image quality and full 3D reconstructions. It does not require administration of iodine contrasts and allows, in a large number of regions, a perfect delimitation of tumor extension. On the other side, MRI has the significant drawback of not providing information on tissue density, so it is hardly usable for dose calculations.

For the described reasons, the combined use of MRI and CT in radiotherapy planning makes interpretation easier, but they are still rarely used in clinical practice, due to lack of compatibility among acquisition devices and planning workstations. Many planning workstations do not allow to use MRI images, nor import predefined contours, and computer image fusion becomes impossible with the standard equipment. To solve this problem, the present work proposes a new simple approach for multimodality integration of MRI information onto CT images for radiotherapy planning. This method allows to transfer segmentation results from MRI to a CT image that will be used for radiotherapy planning using the same original CT format, avoiding the need of any special equipment in the planning workstation.

Multimodality image registration and segmentation processes are carried out on a standard PC workstation. The results are then transferred onto the CT image by slightly modifying up and down the original Hounsfield values of some pixels on the segmented contour. This is enough to see the segmentation result on the CT, but does not affect dose calculations. The CT is then stored using the same file format of the radiotherapy planning workstation, where the technician uses the segmented contour to design the correct beam positioning and doses.

After designing and testing different grids for the MR contour projection on the CT, the developed method has been applied in the radiotherapy planning of five patients, all of them suffering from brain tumors. Image registration, segmentation, grid design and clinical application are described in the following sections.

2. IMAGE REGISTRATION

Several algorithms have been proposed for image registration. The one used in this protocol is based in the maximization of Mutual Information (MI) originally proposed by [8] and [9]. Mutual Information is a concept taken from information theory that represents the degree of dependence of a two random variables A and B by measuring the distance between the joint

distribution $p_{AB}(a,b)$ and the distribution associated with the case of complete independence $p_A(a) \cdot p_B(b)$ [8]. This concept is related to the entropy of the random variables by the equation:

$$I(A,B) = H(A) + H(B) - H(A,B) = H(A) - H(A \mid B) = H(B) - H(B \mid A) \tag{1}$$

where $I(A,B)$ represents the mutual information measurement between A and B, $H(A)$ and $H(B)$ are the entropies of these random variables, $H(A,B)$ their joint entropy, and $H(A/B)$ and $H(B/A)$ the conditional entropies. The entropy provides information on the amount of uncertainty about a random variable, and $I(A,B)$ is the decrease of uncertainty of a random variable A by the knowledge of another variable B. The entropies are calculated as:

$$H(A) = -\sum_a p_A(a) \cdot \log_2 p_A(a) \qquad H(A,B) = -\sum_{a,b} p_{AB}(a,b) \cdot \log_2 p_{AB}(a,b) \tag{2} \tag{3}$$

Working with images, the probability density function is estimated by histogram, usually very easy to obtain. The optimum geometrical transformation T that registers two images will maximize the information of one image that is explained by the other. If B is the image to be transformed and A is the reference, the aim of the algorithm is to find T that maximizes $I(A,T(B))$. Then the calculation of the registration corresponds to the maximization of MI depending on the parameters that describe the transformation. As in our study both images come from the same patient, the registration consists of a rigid body transformation (6 parameters: rotations around the three axis and three translations). For the calculation of the joint histogram we have followed [8], that estimates that joint histogram $H(A,T(B))$ using partial volume interpolation. This interpolation scheme ensures not creating new intensity values in every iteration of the optimization, thus improving the accuracy of the results compared to nearest neighbor or trilinear interpolation.

Optimization is the next step: A multiresolution approach is used for faster and better results. The transformation parameters are calculated with progressive subsampling steps selectable by the user in the range 884, 442, 221, 111 (X, Y and Z subsampling). Steps 442 and 221 were used in all the cases, providing accurate results. The optimization strategy chosen was Simplex method [10] that, according to [11], is a good compromise between speed and simplicity of implementation since it does not require evaluation of the gradient of MI. The solution was found in an average of 2.5 minutes on a standard PC workstation (Intel PIII 800 Mhz, 256 MB RAM). Image dimensions: 320x320x11 (CT), 256x256x11 (MR T2 and PD weighted sequences).
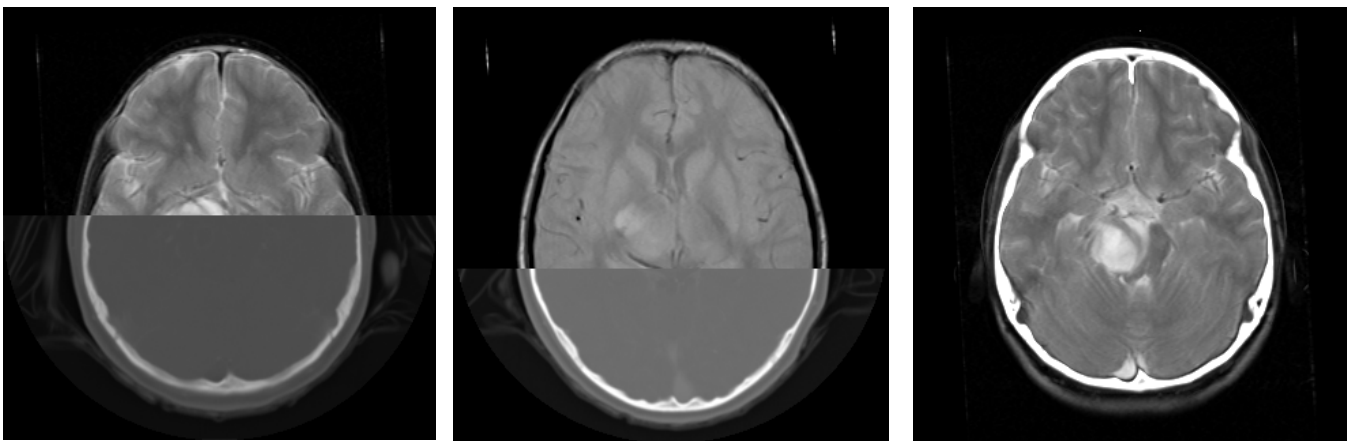

Figure 1. Visualization tools are used in order to check the quality of the registration process. *Curtain mode* shows the continuity between both modalities (CT-MR T2 left, CT-MR PD right). *Maximum mode* (right) combines bone from the CT and soft tissue from the MRI.

This registration method has the advantage of being modality independent, because no assumptions are made about the data values contained in the image. MI algorithm converged to the expected solution in all the studies. The quality of the registration process is checked by displaying both images in a tri-planar viewer and using some other visualization tools (**Figure 1**).

3. IMAGE SEGMENTATION

Once the CT and MRI studies are registered, tumor and other relevant structures are segmented in the MRI image. Several segmentation tools are available for this step: region growing, histogram-based threshold segmentation and pure manual drawing and edition of the contours. Although semiautomatic methods are useful in the segmentation of certain structures, tumors are usually manually outlined because the resulting mask has smoother borders and lower detail, being more adequate for radiotherapy purposes and also easier to transfer onto the CT with the method explained below. Segmentation masks can be overlaid either on the MRI or the CT images (**Figure 2**).
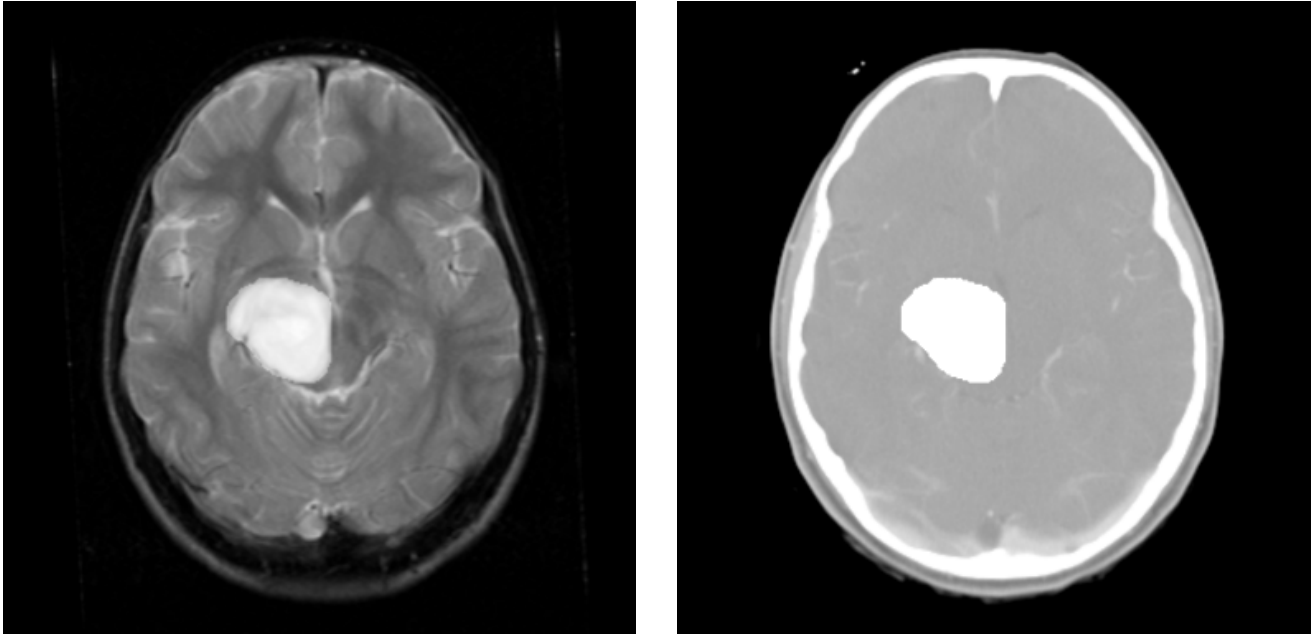

Figure 2. Segmentation is performed on the MR image, where the tumor is easily contoured (left) and can be overlaid on the CT image, since both studies have been previously registered.

4. GRID TYPE SELECTION

The segmented contour must be transferred onto the CT scan keeping the initial image format, which is what the planning workstation understands. This format usually does not allow to include separate contours or annotations. The original values of the CT must be slightly modified in order to incorporate the contour information, but the dose calculations obtained from the CT during the planning process should not change significantly. In order to achieve this goal, the binary contour was multiplied by a grid and then added to the original CT image, resulting in an image similar to the original one but with the segmentation information visible when applying the adequate window level settings. Different settings for this grid have been studied to find the one that produces the smallest modification in the planning dose but still produces conspicuous contours on the modified CT scan.

The process of MR segmentation contour projection on the CT is depicted in **Figure 3**. To project the contour segmented from the MRI on the CT, it is multiplied by a grid and then added to the original CT. This method results in a CT image with small modifications on some of the contour pixels that allow to visualize the tumor segmentation.
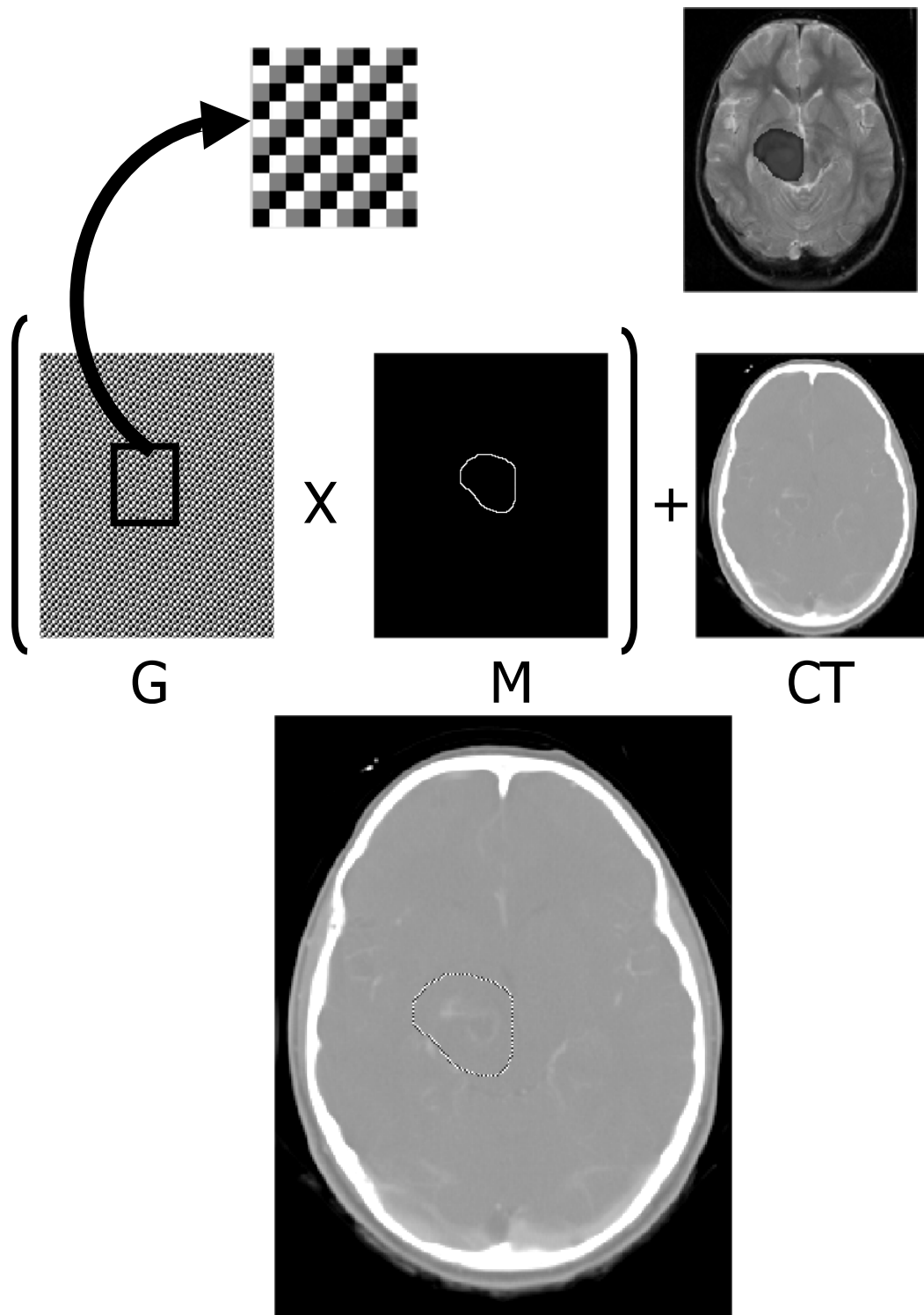
Figure 3. Contour projection process. The tumor is segmented on the MR image, that is registered with the CT (top right). The contour M is multiplied by the grid G, and the result summed to the original CT. The final image with the projected contour is represented at the bottom. (*For display purposes the drawing is exaggerated. With the proper setting the contour is hardly visible on printings*).

The grid consists of a 2D image that multiplies the slices of the segmentation contour, trying to preserve the dose values. This implies that the accumulated values of attenuation along different directions in the modified image must be as similar to the original ones as possible. The different designs tested are depicted on **Figure 4**. Every grid is multiplied by a *displaying factor, D,* and then added to the original image. The factor has been also tested in order to determine the smallest value that allows to display and recognize the contour on the CT image.
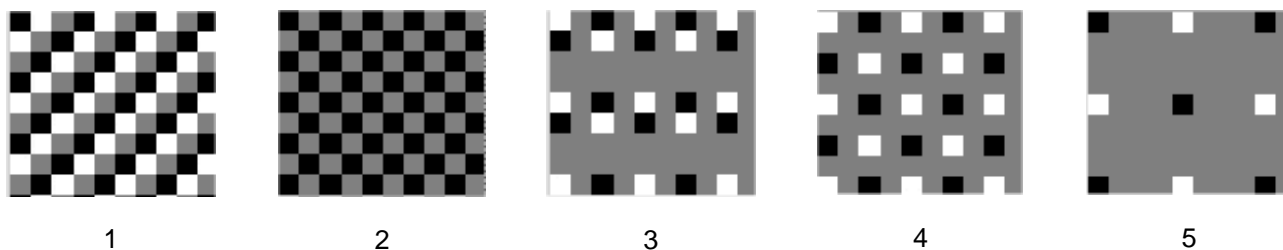

Figure 4. The five grids tested in this study. Black pixels correspond to value 1, gray to value 0 and white to value –1. Grids 1 and 2 try to alternate the modifications in order to preserve the total accumulated values along different directions. Grids 3,4 and 5 include many of pixels equal to zero (gray pixels) in order to modify a lower amount of pixels. This normalized grids are multiplied by the displaying factor D and the summed to the image.

All the grids were tested on one study to find the best one for our purposes. The minimum D factor necessary to correctly distinguish the contour on the CT image was tested by three different users for every grid. The maximum of these three values was used in the tests. To simulate the planning process, the differences between the accumulated attenuation before and after contour projection along several directions were calculated (**Figure 5**). For every grid, the maximum, average and standard deviation of these differences are showed on the following table:

Table 1. Maximum, average and standard deviation of the difference between the accumulated attenuations in the original and modified images along different directions. Results for grid 5 are not presented, as no user was able to distinguish the contour on the CT image when applying this grid. It was not longer used.

	Grid 1, D=10	Grid 2, D=10	Grid 3, D=20	Grid 4, D=20
Max (%)	0,2539	0,24449	0,5521	0,5021
Average (%)	0,1776	0,1683	0,3137	0,3265
Std. Dev. (%)	0,0359	0,03465	0,0966	0,0838

These results show that grids 1 and 2 produce the lowest differences in attenuation. Grids 3 and 4 have many coefficients equal to zero, and consequently the contour has less pixels than when using grids 1 and 2. This requires a higher D value to distinguish the segmentation. The best grids are then 1 and 2, and among them it was easier for the three users to distinguish the contour with grid number 2, that was then the one selected for the clinical application of the method.
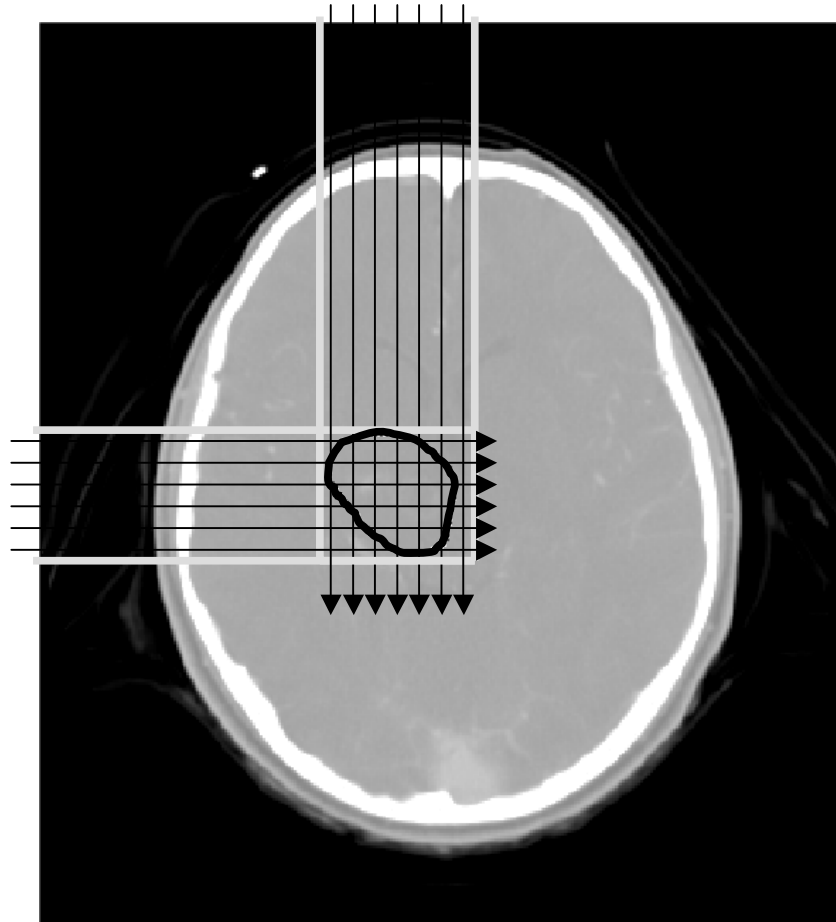
Figure 5. The planning process is simulated in the modified CT image in order to calculate the differences in attenuation introduced by the proposed grids. For simplicity of the figure, only two of the directions used are showed for a particular slice, although four directions were used (two vertically and two horizontally). Both in the original and modified CT the pixel values are summed from the image border to the end of the tumor contour, to reproduce the radiotherapy process, and then compared.

5. CLINICAL APPLICATION

The method proposed for MRI segmentation and projection onto the CT has been clinically tested on five brain tumor patients. Usually this pathology is not well visualized on CT images, nor it shows its real extension, while it is easily distinguished on the MR images.

T2 and PD weighted MR images were acquired on a Philips GyroScan ACS 1.5 T, and CT scans on a Philips LX Scanner. Both studies were transmitted through the hospital network to the physician's PC workstation, where they were registered using our implementation of the MI algorithm. The tumor was then segmented on the MRI by the physician, and then converted into a contour visible on the CT using the procedure described in the previous section. Variations of CT image along the contour are so slight that it is only observed when using the proper window-level settings, (**Figure 6**). The resulting image was transmitted to the planning workstation, where the technician was able to distinguish the segmented contour of the segmented structures, with the proper window level settings. Therapy planning was then performed taking benefit from this information, not originally present on the CT.
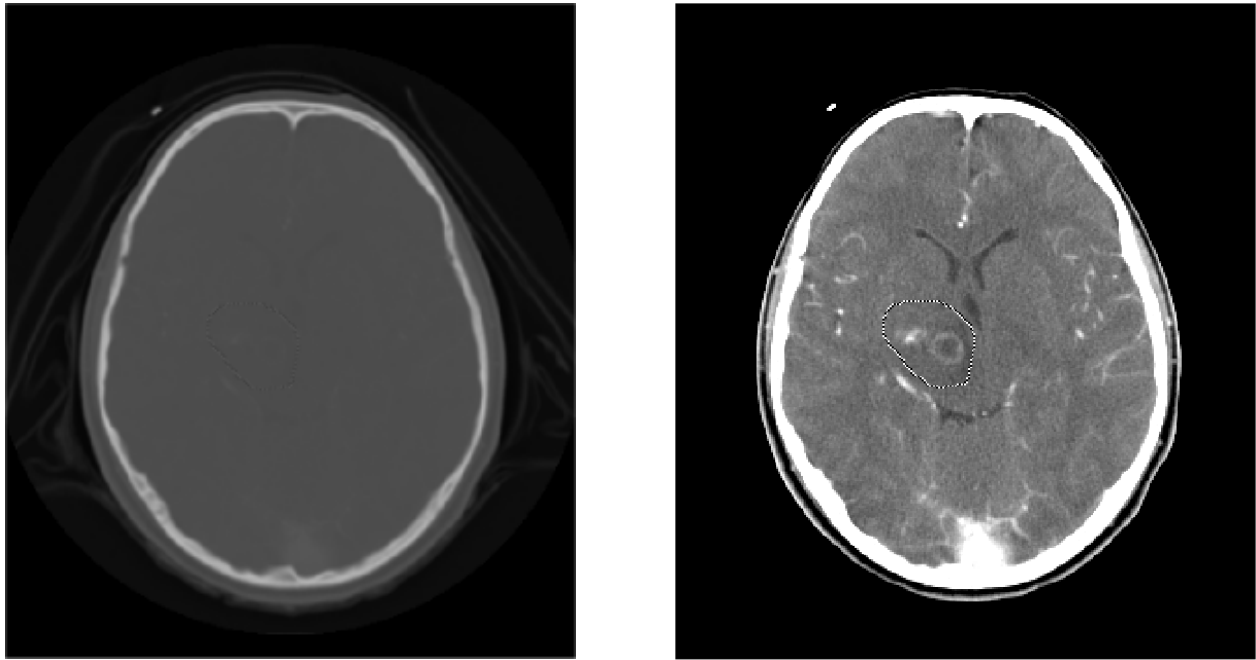
Figure 6. The segmented contour is only visible with the correct window level settings (right) as the original CT values have been modified very slightly.

The physicians and the therapy planning technicians reported a significant improvement when using the described method, compared to the conventional radiotherapy planning using only the CT scan. The facility of registering and segmenting the images on a standard PC workstation provided several advantages for the radiation oncologist, as he/she can perform all the process in the office without the need of being present during the planning session to indicate the limits of the tumor. The registering process was not used in the previous method, and the physician needed to visually compare hardcopies of the MRI and the CT. These images have usually significant difference in rotation between them, producing slices that are not easily comparable.

Other methods exist that provide multimodality image visualization for planning workstations [7, 12]. The protocol described in this paper tries to introduce multimodality facilities in a regular planning workstation not able to accept other images than the CT scan and to separate the tasks that the physician can carry out on his/her own from the technician tasks.

Further work includes the application of the proposed method to images from other part of the body, like abdomen or pelvis, where other indications like prostate cancer would be benefited. The extension of the protocol to these areas has to face two main problems: registration process and attenuation issues. While the head and the brain are assumed not to move between different image acquisitions, other parts of the body do not behave in that way. The patient position has to be carefully considered in order to achieve a successful registration afterwards. Non-rigid registration methods could be necessary for this step. The diverse composition of these areas of the body in terms of bone and soft tissue would have to be also studied to assure that the described grid does not modify attenuation profiles in these images either.

The technique proposed in this article has proven to be easy to use for the radiation oncologists and allows them to separate the segmentation and planning processes. The introduction of tumor contours taken from MR images improves the accuracy of the radiotherapy planning without requiring expensive multimodality 3D planning workstations.

ACKNOWLEDGEMENTS

6. REFERENCES

1. C. A. Perez, J. M. Michalski, J. A. Purdy, T. H. Wasserman, K. Williams, and M. A. Lockett, "Three-dimensional conformal therapy or standard irradiation in localized carcinoma of prostate: preliminary results of a nonrandomized comparison," *Int J Radiat Oncol Biol Phys*, **47**, pp. 629-37, 2000.

2. J. M. Michalski, J. A. Purdy, K. Winter, M. Roach, 3rd, S. Vijayakumar, H. M. Sandler, A. M. Markoe, M. A. Ritter, K. J. Russell, S. Sailer, W. B. Harms, C. A. Perez, R. B. Wilder, G. E. Hanks, and J. D. Cox, "Preliminary report of toxicity following 3D radiation therapy for prostate cancer on 3DOG/RTOG 9406," *Int J Radiat Oncol Biol Phys*, **46**, pp. 391-402, 2000.

3. C. C. Ling, J. Humm, S. Larson, H. Amols, Z. Fuks, S. Leibel, and J. A. Koutcher, "Towards multidimensional radiotherapy (MD-CRT): biological imaging and biological conformality," *Int J Radiat Oncol Biol Phys*, **47**, pp. 551-60, 2000.

4. M. S. Rudoltz, K. Ayyangar, and M. Mohiuddin, "Application of magnetic resonance imaging and three-dimensional treatment planning in the treatment of orbital lymphoma," *Med Dosim*, **18**, pp. 129-33, 1993.

5. S. L. Sailer, J. G. Rosenman, M. Soltys, T. J. Cullip, and J. Chen, "Improving treatment planning accuracy through multimodality imaging," *Int J Radiat Oncol Biol Phys*, **35**, pp. 117-24, 1996.

6. V. S. Khoo, E. J. Adams, F. Saran, J. L. Bedford, J. R. Perks, A. P. Warrington, and M. Brada, "A Comparison of clinical target volumes determined by CT and MRI for the radiotherapy planning of base of skull meningiomas," *Int J Radiat Oncol Biol Phys*, **46**, pp. 1309-17, 2000.

7. H. Y. Lau, K. Kagawa, W. R. Lee, M. A. Hunt, A. H. Shaer, and G. E. Hanks, "Short communication: CT-MRI image fusion for 3D conformal prostate radiotherapy: use in patients with altered pelvic anatomy," *Br J Radiol*, **69**, pp. 1165-70, 1996.

8. F. Maes, A. Collignon, D. Vandermeulen, G. Marchal, and P. Suetens, "Multimodality image registration by maximization of mutual information," *IEEE Trans Med Imaging*, **16**, pp. 187-98, 1997.

9. W. M. Wells, P. Viola, H. Atsumi, S. Nakajima, and S. Kikinis, "*Multi-modal volume registration by maximization of mutual information*," *Medical Image Analysis*, **1**, pp. 35-51, 1996/97.

10. W. H. Press, S. A. Teukolsky, W. T. Vetterling, and B. P. Flannery, *Numerical Recipes in C*, Second ed: Cambridge University Press, 1992.

11. F. Maes, D. Vandermeulen, and P. Suetens, "Comparative evaluation of multiresolution optimization strategies for multimodality image registration by maximization of mutual information," *Med Image Anal*, **3**, pp. 373-86, 1999.

12. K. Schubert, F. Wenz, R. Krempien, O. Schramm, G. Sroka-Perez, P. Schraube, and M. Wannenmacher, "[Possibilities of an open magnetic resonance scanner integration in therapy simulation and three-dimensional radiotherapy planning]," *Strahlenther Onkol*, **175**, pp. 225-31, 1999.